# LACK OF SUBSOLIDUS REE EXCHANGE BETWEEN PYROXENE AND PHOSPHATE IN THE RODA DIOGENITE

G.W. Fowler[1], D.W. Mittlefehldt[2], J.J. Papike[1], and M.N. Spilde[1]. [1]Institute of Meteoritics, Department of Earth & Planetary Sciences, University of New Mexico, Albuquerque, NM 87131, U.S.A. [2]C23, Lockheed Martin ESS, 2400 Nasa Road 1, Houston, TX 77058, U.S.A.

*INTRODUCTION*.  Roda is an achondrite meteorite classified as a diogenite. Diogenites, along with eucrites and howardites, are believed to have originated on asteroid 4 Vesta during an extensive melting event at ~ 4.6 b.y. [1]  In general diogenites are composed of > 90% pyroxene with minor olivine and chromite, and trace amounts of plagioclase, silica, metal, troilite and phosphate [2].  The orthopyroxene phase of the diogenites has been extensively studied [2,3,4] in hopes of finding clues to the petrogenesis of the howardite, eucrite, diogenite (HED) parent body.  Mittlefehldt [2] used INAA on orthopyroxene separates while Fowler et al. [4] used SIMS techniques on orthopyroxene in thin sections.  In the course of these studies it was noted that Roda was a compositional outlier due to its extreme range in trace elements.  The ranges of REE found in Roda by [2] and [4] were as large or larger than the range of the entire suite of other diogenites.  Most diogenites show a finite but limited range of trace elements.  The extreme range of trace element concentrations in Roda might be explained by the diffusion of these elements into orthopyroxene from a phosphate or trapped melt phase.  We test this theory in this study.

*RESULTS AND DISCUSSION*.  We have measured 6 REE, Sr, Y, and Zr in 5 locations on Roda OPX grain 15, Table 1.  Figure 1 shows a BSE image of Roda grain 15 with the five SIMS pits clearly visible.  EMP analyses of this grain by Mittlefehldt [2] indicate that LREE-rich phosphates (white) are enclosed in clinopyroxene (light gray) exsolved from orthopyroxene (medium gray).  A Si-Al-K- and Ba rich glass is also present (dark gray) enclosed in the orthopyroxene.  Locations R15-1, R15-3, and R15-4 are in the orthopyroxene phase, and R15-2 and R15-5 are in the clinopyroxene phase.  Figure 2 shows the corresponding REE analyses for these pits along with the average Roda orthopyroxene analysis taken from Fowler et al. [4].  Gd has been estimated using an interpolation between Dy and Sm.  There appears to be no significant difference in REE between the core of the grain (R15-1) and the area next to the clinopyroxene and near the phosphate and glass (R15-3).  The light REE from the orthopyroxene phase of this grain are very close to the average given by Fowler et al. [4].  There is a slight difference in the light REE for the two clinopyroxene analyses and no difference in the heavy REE.  Therefore the phosphate inclusions in exsolved clinopyroxene in the orthopyroxene host do not appear to explain the large ranges of trace element composition in the Roda diogenite.  It appears that Roda is a polymict breccia sampling a variety of lithologies with diverse compositions.  However, the trace element enriched Roda subsamples represent cumulate orthopyroxenites that crystallized from melts more evolved and thus enriched in incompatible trace elements relative to most other diogenites.

*REFERENCES.*  [1] Consolmagno and Drake (1977) G.C.A., 41, 1271-1282.  [2] Mittlefehldt (1994) G.C.A., 58, 1537-1552.  [3] Fowler et al. (1994) G.C.A., 58, 3921-3929.  [4] Fowler et al. (1995), G.C.A. 59, 3071-3084.
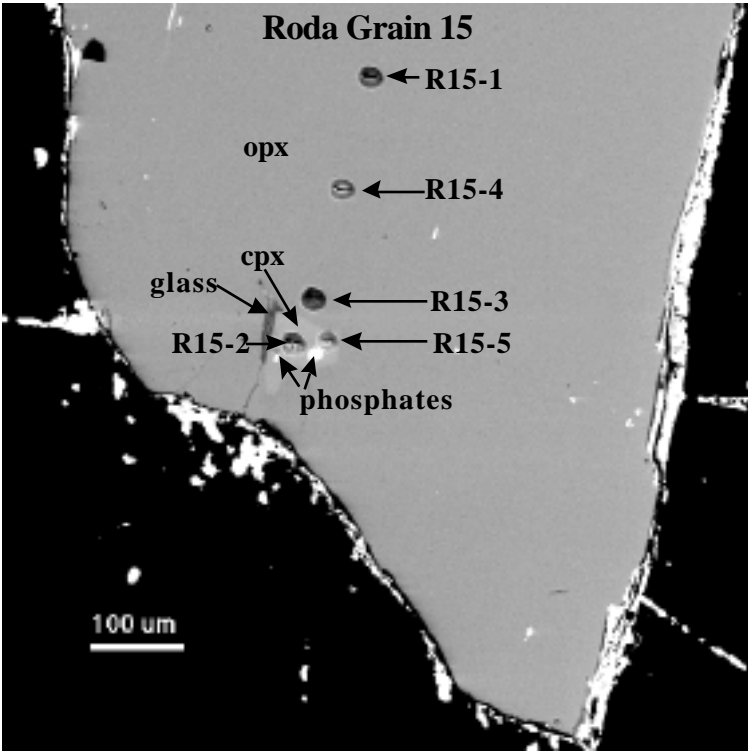
## Figure 1



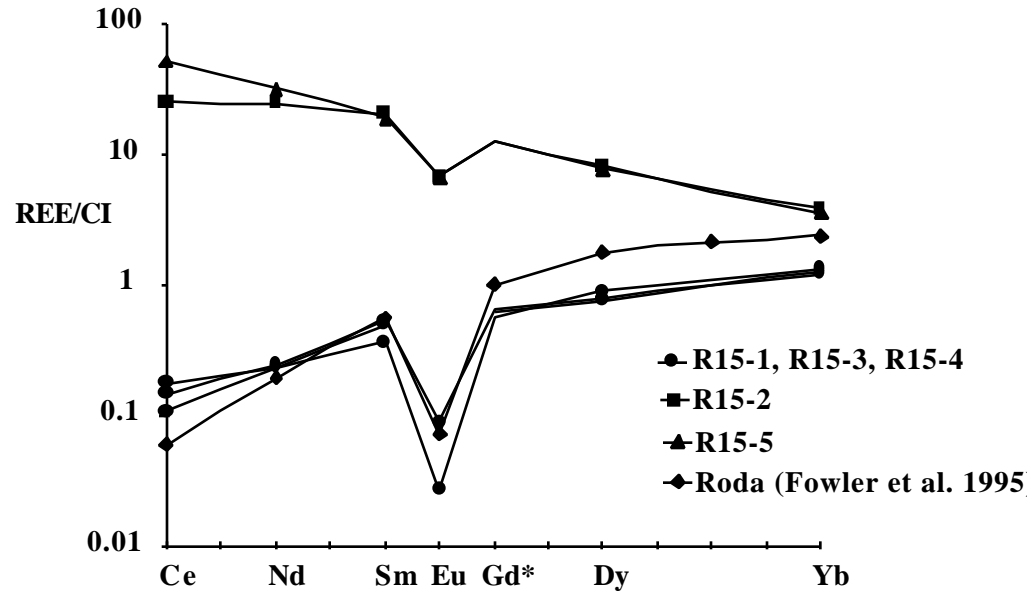Roda Grain 15

## Figure 2



Table 1. SIMS analyses of Roda grain 15.

| Analysis | Sr (ppm) | Y | Zr | Ce | Nd | Sm | Eu | Dy | Yb |
|---|---|---|---|---|---|---|---|---|---|
| R15-1 | 0.04 | 1.94 | 3.74 | 0.11 | 0.11 | 0.05 | 0.00 | 0.21 | 0.22 |
| R15-2 | 30.40 | 9.78 | 33.69 | 15.52 | 11.43 | 3.06 | 0.37 | 1.99 | 0.63 |
| R15-3 | 0.04 | 1.69 | 2.44 | 0.09 | 0.11 | 0.08 | 0.00 | 0.19 | 0.20 |
| R15-4 | 0.03 | 1.68 | 3.07 | 0.06 | 0.11 | 0.07 | 0.01 | 0.19 | 0.21 |
| R15-5 | 20.20 | 9.24 | 30.66 | 32.07 | 14.89 | 2.86 | 0.31 | 1.91 | 0.58 |

b.d. = below detection